



Crystal structure and phase transition in the compound



HibaKhili^a, Najla Chaari^a, Abdelaziz Koumina^b, Slaheddine Chaabouni^a.

^a Laboratoire des Sciences des Matériaux et de l'Environnement, département de chimie, Faculté des Sciences de Sfax, BP 1171, 3018 Sfax, Tunisia.

E-mail address: Kh.Hiba@hotmail.com; n_chaari2003@yahoo.fr;
chaabouni_slaheddine@yahoo.fr.

^b ENS de Marrakech, Département de physique, Université Cadi-Ayyad Marrakech, Morocco.
E-mail address: koumina@gmail.com.

Abstract

The title compound 1-(2-ammonium-ethyl) piperaziniumpentachlorothallate (III) dihydrate crystallizes in the monoclinic system with space group Cm. The unit cell dimensions are: $a = 12.786(5)$, $b = 12.021(5)$, $c = 10.566(5)$ Å, $\beta = 93.469(5)^\circ$, with $Z = 4$. Its crystal structure was determined and refined down to $R = 0.045$. The structure of this compound consists of 1-(2-ammonium-éthyl) pipéraziniumcations and $[\text{Ti}_2\text{Cl}_{10}]^{4-}$ dimers. The arylammoniumcations are located between anions and connected to the halogen atoms by N-H...Cl hydrogen bonds. One phase transition at $T = 320$ K is detected and studied by differential scanning calorimetry, dielectric and impedance spectroscopy measurements. The evolution of the dielectric constant and dissipation factor as a function of temperature revealed the transition characterized by a strong jump in the conductivity plot.

Keywords:

Organic-inorganic hybrid material; Crystal structure; Halogenothallates(III).

*Corresponding author: Hiba Khili.

Tel: +21698813420, fax +21674274437

E-mail address: kh.hiba@hotmail.com

Address: Route de Soukra km 3.5 - B.P. n° 1171 - 3000 Sfax.

Council for Innovative Research

Peer Review Research Publishing System

Journal: Journal of Advances in Chemistry

Vol. 8, No. 1

editor@cirworld.com

www.cirworld.com, member.cirworld.com



I. Introduction

A large number of inorganic thallium (III) complexes are presently known and a systematic survey of their main crystallographic data has been reported [1, 2]. Thallium complexes exhibit a wide range of coordination numbers and geometries (tetrahedral [4, 5, 6], square pyramidal [6, 7], trigonalbipyramid [3, 5], octahedral [5, 7]) and the empirical formula of the complex is not always a reliable indicator for its structure. Some of these compounds exhibit structural phase transitions and interesting physical properties such as ferroelectricity and ionic conduction [8, 9].

Recently, the research of organic-inorganic polar crystals is very important for quadratic nonlinear optical phenomena which are, today, oriented to the organic aromatic cations containing π -electrons systems asymmetricized by electron donor and/or accepted substitutes.

The second is devoted to the ionic hostmatrices that may increase the packing cohesion built up through ionic, hydrogen bonding often by underlying of a more important resistance in organic-inorganic polar crystals than in purely organic polar materials. Taking these considerations into account, we report and discuss the results of investigations, concerning a new compound $[\text{C}_6\text{H}_{17}\text{N}_3]\text{TlCl}_5 \cdot 2\text{H}_2\text{O}$. We have performed X-ray diffraction measurements providing us information about the complete crystal structure at room temperature. This structural study is accompanied by calorimetric, dielectric and impedance spectroscopy measurements.

II. Experimental section

II.1. Crystal chemistry

1-(2-ammonium-éthyl) piperaziniumpentachlorothallate (III) dihydrate crystals were obtained by dissolving the appropriate amine and Tl_2O_3 in a minimum volume of concentrated hydrochloric acid, warming as necessary. After several weeks of evaporation, parallelepiped shaped monocrystals were obtained and these were isolated by filtration and dried in a vacuum desiccator. The chemical analysis of thallium atoms and chloride anions has been carried out [10]. Density was measured at room temperature by flotation in CCl_4 . It is noted that the compound is stable in air and its formula is determined by chemical analysis and confirmed by refinement of the crystal structure. The average value of density, $D_m = 2.211 \text{ g cm}^{-3}$, is in agreement with that calculated, $D_x = 2.198 \text{ g cm}^{-3}$. The cell contains four formula units of $[\text{C}_6\text{H}_{17}\text{N}_3]\text{TlCl}_5 \cdot 2\text{H}_2\text{O}$.

II.2. Crystal structure

The single crystal study was performed by using a four-circle Bruker APEXII CCD diffractometer. The main crystal data, the parameters used for intensity data collection and the reliability factors are summarized in Table 1. The crystal structure was carried out with a Patterson method using SHELXS-86 [11] which allowed the localization of thallium and chlorine atoms.

All the other atoms were located after subsequent cycles of refinement and difference-Fourier syntheses by using SHELXL-97 [12]. All H-atoms positions could be determined from the difference Fourier map. However, the calculated positions at a distance of 0.96 were used in the final refinement, with a common isotropic displacement parameter, since the calculated distances were more reasonable than the refined ones. Full matrix refinement with anisotropic thermal parameters for all non hydrogen atoms and isotropic thermal parameters for H atoms converged to a final R value of 0.045.

**Table 1. Summary of physical constants and parameters associated with data collection and structure refinement**

Compound	1-(2-ammonium-ethyl) piperaziniumpentachlorothallate (III) dihydrate
Formula	[C ₆ H ₁₇ N ₃] ⁺ TlCl ₅ ·2H ₂ O
Color/shape	Colorless/parallelepiped
System	Monoclinic
Space group	Cm
Temperature (°C)	25
Cell constants	
a(Å)	12.786(5)
b(Å)	12.021(5)
c(Å)	10.566(5)
β (°)	93.469 (5)
Cell volume (Å ³)	1621.0 (1)
Formula units/unit cell	4
Formula weight	1627.12
D _{calc} (g cm ⁻³)	2.198
D _{obs} (g cm ⁻³)	2.211
Diffractometer/scan	Bruker APEXII CCD
Radiation, graphite monochromator	Mo Ka (k = 0.71073 Å ⁻¹)
Crystal dimensions (mm)	0.01 x 0.02 x 0.03
Absorption	Numerical
μ _{calc} (mm ⁻¹)	35.27
Unique reflections	1302
θ range (deg)	3.5 ≤ θ ≤ 35°
Reflections with I > 4σ(F _o)	1222
Range of h, k, l	±11, ±10, ±9
F(000)	1680.0
R = Σ F _o - F _c / Σ F _o	0.045
R _w	0.051
Number of parameters	164
Computer programs	SHELXS [10], SHELXL [11]

The final atomic coordinates are given in Table 2. Main geometrical features, bond distances and angles are reported in Table 3. Hydrogen bonding parameters are reported in Table 4.

II.3. Calorimetric measurements

DSC experiments were performed on heating the 1-(2-ammonium-ethyl) piperaziniumpentachlorothallate (III) dihydrate from 193 K to 373 K. The DSC measurements were performed with the heating/cooling rates at a heating rate of 5 K.min⁻¹.

II.4. Electrical measurements

Crystals of $[\text{C}_6\text{H}_{17}\text{N}_3]\text{TlCl}_5 \cdot 2\text{H}_2\text{O}$ were crushed and pressed to dense and translucent pellets (8mm in diameter ; 2 mm in thickness) at a pressure of 200 MPa. Both planar faces of these pellets were coated with silver paint and the pellets were then sandwiched between metal electrodes, which were also coated with silver paint. Electrical properties were determined by impedance method using a frequency response analyzer Novocontrol BDS 400. The frequency range was 1 Hz–1MHz and the measurements were carried out in vacuum between 298 and 413 K. The sample temperature was stabilized at $\pm 5^\circ\text{C}$.

III. Result and discussions

III.1. Crystallography study

$[\text{C}_6\text{H}_{17}\text{N}_3]\text{TlCl}_5 \cdot 2\text{H}_2\text{O}$ belongs to a monoclinic Cm space group at 298 K. The structural study of the compound $[\text{C}_6\text{H}_{15}\text{N}_3]\text{TlCl}_5 \cdot 2\text{H}_2\text{O}$ revealed that the coordination polyhedra of thallium is formed by association of two octahedral sharing two chlorine vertices (an edge) forming dimers along the a axis. These dimers are arranged around $z = 0$.

A projection along the b axis of the atomic arrangement of $[\text{C}_6\text{H}_{17}\text{N}_3]\text{TlCl}_5 \cdot 2\text{H}_2\text{O}$ is depicted in Figure 1. The structure of the title compound consists of $[\text{Tl}_2\text{Cl}_{10}]^{4-}$ dimer anions and biprotonated 1-(2ammonium-ethyl) piperazinium cations, the TlCl_6^{3-} configuration is a slightly distorted octahedron.

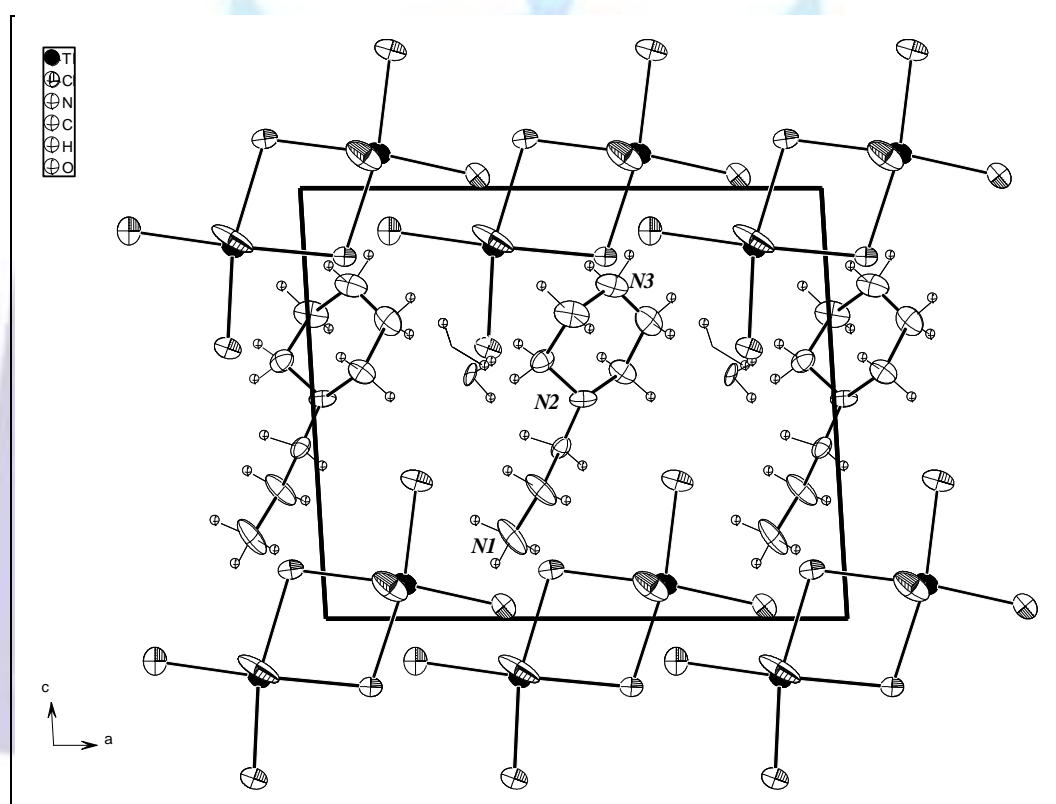


Fig1: Projection of $[\text{C}_6\text{H}_{17}\text{N}_3]\text{TlCl}_5 \cdot 2\text{H}_2\text{O}$ structure in the (a,c) plane.

Each thallium ion is surrounded by six chlorine ions and the Tl–Cl bond lengths ranging from 2.392(1) to 2.806(2) Å. The angles involving mutually cis ions range from 78.6(4) to 98.4(5) °, while the trans angles vary from 164.2(4) to 176.9(6) °.

The deviations of these bond angles from the ideal values of 90° and 180° are consistent with the presence of the long bonds, the largest deviations from 90° involving the most weakly bonded chlorine ions, $\text{Cl}_3\text{–Tl}_1\text{–Cl}_4 = 79.2(4)^\circ$, $\text{Cl}_3\text{–Tl}_2\text{–Cl}_4 = 78.6(4)^\circ$, $\text{Cl}_4\text{–Tl}_1\text{–Cl}_7 = 82.4(2)^\circ$. Table 3 reports the main geometrical features of 1-(2 ammonium-ethyl) piperazinium entities. The organic groups are located in the (a, c) plane around $z = 0.5$.

The C–N bond lengths vary from 1.37(3) to 1.50(4) Å. The C–C bond lengths vary from 1.51(3) to 1.63(4) Å. They are in agreement with those found in the related compounds [13–14]. The C–C perpendicular interplanar distances range from 6.397(3) Å and 6.963(3) Å, indicating the existence of Van der Waals interactions between $[\text{C}_6\text{H}_{17}\text{N}_3]^+$ cations.



Table 2. The final atomic coordinates

Atoms	X/a	Y/b	Z/c	U_{eq} or U_{iso} *
Tl1	0.1521(3)	0.0000	0.0836(3)	0.0384
Tl2	-0.1381(3)	0.0000	-0.1322(3)	0.0354
Cl1	0.3406(1)	0.0000	0.0316(1)	0.0785
Cl2	0.1884(1)	0.0000	0.3234(1)	0.0419
Cl3	0.0761(1)	0.0000	-0.1564(1)	0.0491
Cl4	-0.0639(1)	0.0000	0.1168(1)	0.0363
Cl5	-0.1591(1)	0.0000	-0.3690(1)	0.0401
Cl6	-0.3350(1)	0.0000	-0.0968(2)	0.0948
Cl7	0.1248(7)	0.2099(8)	0.0779(1)	0.0595
Cl8	-0.1371(8)	0.1984(8)	-0.1148(1)	0.0665
N1	0.3653(2)	0.266(2)	0.193(2)	0.0606
C1	0.426(2)	0.212(2)	0.302(3)	0.0539
C2	0.4690(2)	0.295(2)	0.400(2)	0.0258
N2	0.5172(2)	0.2412(1)	0.5134(1)	0.0248
C3	0.596(2)	0.3241(2)	0.576(2)	0.0353
C4	0.652(2)	0.256(2)	0.694(3)	0.0420
N3	0.5856(2)	0.2103(2)	0.7765(2)	0.0423
C5	0.505(2)	0.1352(2)	0.710(2)	0.0421
C6	0.4432(2)	0.1982(2)	0.601(2)	0.0323
O1	0.7709(1)	0.5000	0.6347(1)	0.0094
O2	0.8037(1)	0.328(2)	0.5700(1)	0.0912
H1-1	0.3332	0.2254	0.1275	0.0824
H1-2	0.4105	0.3312	0.1591	0.0824
H1-3	0.2999	0.3204	0.2279	0.0824
H11	0.3673	0.1675	0.3428	0.0660
H12	0.4755	0.1686	0.2728	0.0660
H21	0.5118	0.3443	0.3536	0.0341
H22	0.4043	0.3415	0.4252	0.0341
H31	0.6504	0.3473	0.5144	0.0438
H32	0.5613	0.3924	0.6061	0.0438
H41	0.7019	0.3064	0.7440	0.0498
H42	0.6943	0.1926	0.6596	0.0498
H3-1	0.6263	0.1660	0.8430	0.0511
H3-2	0.5481	0.2722	0.8187	0.0511
H51	0.4544	0.1070	0.7709	0.0531
H52	0.5410	0.0699	0.6716	0.0531
H61	0.4029	0.2616	0.6370	0.0411
H62	0.3913	0.1467	0.5548	0.0411
H1W1	0.7608	0.5697	0.6844	0.0149
H1W2	0.8355	0.5000	0.5867	0.0149
H2W1	0.8482	0.3934	0.5974	0.1078
H2W2	0.8438	0.2807	0.5111	0.1078

**Table 3. Main interatomic distances (Å) and bond angles (deg) in [C₆H₁₇N₃] TlCl₅ · 2H₂O.**

Organic group			
N3 - C4	1.37(3)	C4-N3-C3	112.1(2)
N3 - C5	1.51(3)	N2-C3-C4	104.5(2)
C3 - N2	1.54(3)	C3-N2-C6	113.2(2)
C3 - C4	1.63(4)	C3-N2-C2	107.5(1)
N2 - C6	1.46(3)	C6-N2-C2	114.7(2)
N2-C2	1.47(3)	C3-C4-N3	115(2)
C5-C6	1.56(3)	N3-C3-C6	110.9(2)
C1-N1	1.50(4)	C3-C6-N2	108.6(2)
C1-C2	1.51(3)	N1-C1-C2	112(2)
O1-H1W1	1.002	C1-C2-N2	112.5(2)
O1-H1W2	0.994		
O2-H2W1	1.003		
O2-H2W2	1.006		

[TlCl₆]³⁻ octahedron 1

<i>Tl1</i>	<i>Cl1</i>	<i>Cl2</i>	<i>Cl3</i>	<i>Cl4</i>	<i>Cl7</i>	<i>Cl7'</i>
<i>Cl1</i>	2.504(2)	3.748(7)	3.974(9)	5.374(7)	3.655(7)	3.655(7)
<i>Cl2</i>	95.7(5)	2.548(2)	5.192(7)	3.691(8)	3.622(6)	3.622(7)
<i>Cl3</i>	95.3(5)	169.1(5)	2.661(2)	3.535(9)	3.617(6)	3.617(6)
<i>Cl4</i>	174.5(5)	89.8(5)	79.2(4)	2.806(2)	3.705(8)	3.705(1)
<i>Cl7</i>	97.3(2)	92.3(3)	86.3(3)	82.4(2)	2.548(2)	5.027(6)
<i>Cl7'</i>	97.3(2)	92.3(3)	86.3(3)	82.4(2)	164.2(4)	2.548(1)

[TlCl₆]³⁻ octahedron 2

<i>Tl2</i>	<i>Cl3</i>	<i>Cl4</i>	<i>Cl5</i>	<i>Cl6</i>	<i>Cl8</i>	<i>Cl8'</i>
<i>Cl3</i>	2.766(2)	3.535(7)	3.695(1)	5.318(7)	3.524(7)	3.524(8)
<i>Cl4</i>	78.6(4)	2.742(2)	5.231(7)	3.912(7)	3.506(7)	3.506(7)
<i>Cl5</i>	87.4(5)	166.0(4)	2.500(2)	3.783(7)	3.644(7)	3.644(7)
<i>Cl6</i>	176.9(6)	98.4(5)	95.7(5)	2.568(2)	3.690(8)	3.690(9)
<i>Cl8</i>	90.4(3)	85.8(3)	94.4(3)	89.4(3)	2.392(1)	4.870(7)
<i>Cl8'</i>	90.4(3)	85.8(3)	94.4(3)	89.4(3)	171.2(6)	2.392(1)

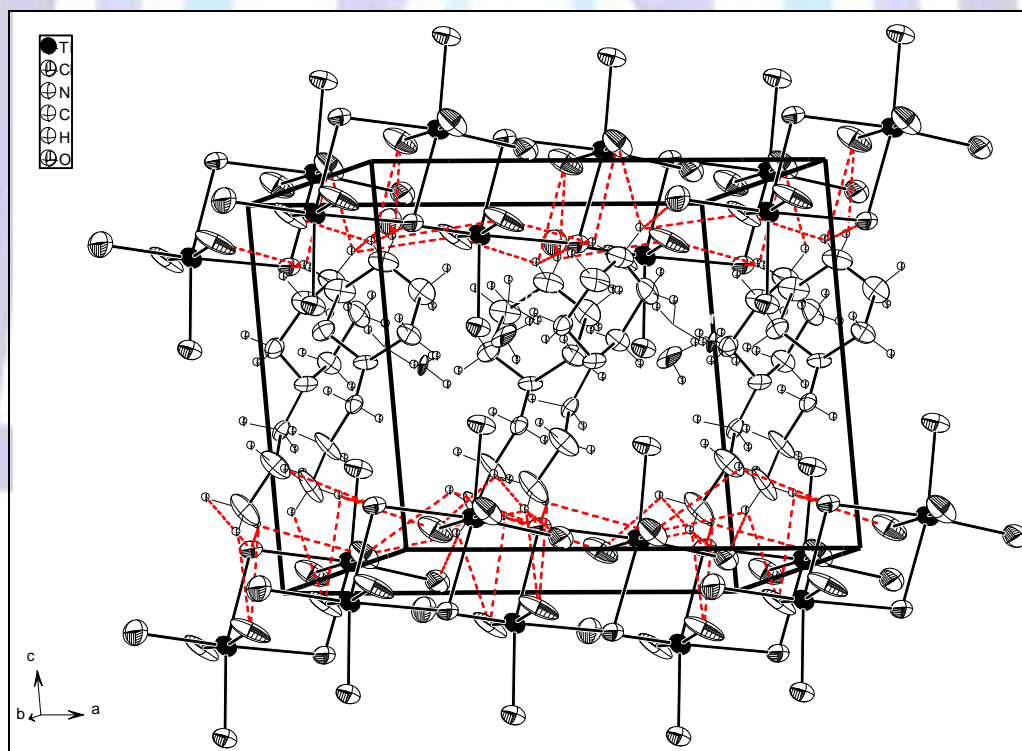
The intermolecular hydrogen bonding contacts N-H...Cl provide a linkage between the [C₆H₁₇N₃]²⁺ entities and the [Tl₂Cl₁₀]⁴⁻ anions figure 2.

The hydrogen bonds give rise to a three-dimensional construction of the structure and add stability to this compound.

Table 4. Hydrogen bonding parameters for $[\text{C}_6\text{H}_{15}\text{N}_3] \text{TiCl}_5 \cdot 2\text{H}_2\text{O}$

N-H...Cl	d(D-H)	d(H...A)	<DHA	d(D...A)
N1-H1-1...Cl1	0.923(2)	2.896(5)	137.29(1)	3.629(2)
N1-H1-1...Cl7	0.923(2)	2.691(9)	124.96(1)	3.307(3)
N1-H1-1...Cl8 ^(a)	0.923(2)	2.767(1)	116.05(1)	3.279(2)
N1-H1-2...Cl4 ^(b)	1.05(2)	2.108(4)	152.51(1)	3.077(3)
N1-H1-2...Cl7 ^(b)	1.05(2)	2.962(1)	120.83(1)	3.614(3)
N1-H1-2...Cl8 ^(a)	1.05(2)	2.943(1)	99.2(1)	3.279(2)
N1-H1-3...Cl4 ^(b)	1.14(2)	3.053(1)	80.48(1)	3.077(3)
N1-H1-3...Cl7	1.14(3)	2.976(1)	96.58(2)	3.307(3)
N3-H3-1...Cl6 ^(c)	1.002(2)	2.143(6)	143.49(1)	3.008(2)
N3-H3-1...Cl7 ^(d)	1.002(2)	2.897(1)	107.28(1)	3.335(2)
N3-H3-1...Cl8 ^(c)	1.002(2)	3.056(1)	120.14(1)	3.663(2)
N3-H3-2...Cl3 ^(e)	1.004(2)	2.772(3)	135.38(1)	3.557(2)
N3-H3-2...Cl7 ^(d)	1.004(2)	2.861(1)	109.61(1)	3.335(2)
N3-H3-2...Cl8 ^(d)	1.004(2)	2.535(1)	134.87(1)	3.321(2)

Symmetry code: ^(a): (0.5+x, 0.5-y, z); ^(b): (0.5+x, 0.5+y, z); ^(c): (1+x, y, 1+z); ^(d): (0.5+x, 0.5-y, 1+z); ^(e): (0.5+x, 0.5+y, 1+z)


 Fig 2: A perspective drawing of $[\text{C}_6\text{H}_{17}\text{N}_3] \text{TiCl}_5 \cdot 2\text{H}_2\text{O}$ structure. The broken lines show the hydrogen bonding.



III.2. Infrared spectroscopy

As IR spectroscopy is one of the major physical methods of investigation of the molecular structure, we have studied the infrared spectrum of the title compound. IR spectra of this compound have been investigated in the frequency range 400–4000 cm^{-1} . The frequencies of infrared peaks are quoted in Table 5.

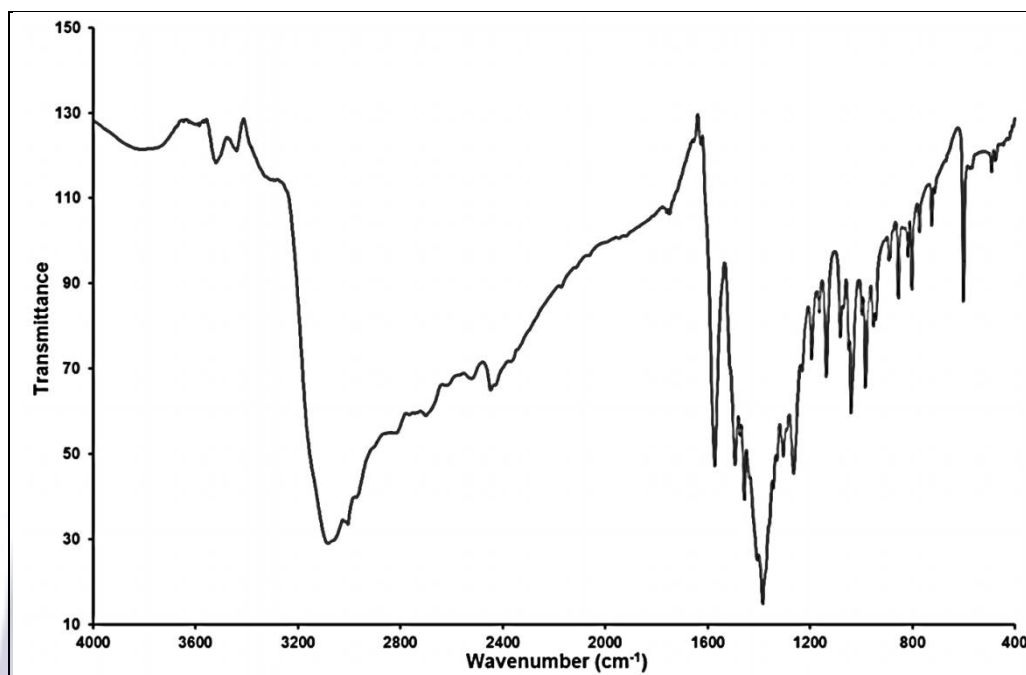


Fig 3: Infrared absorption spectrum of $[\text{C}_6\text{H}_{17}\text{N}_3] \text{TICl}_5 \cdot 2\text{H}_2\text{O}$.

Both absorption bands appearing at 3813 cm^{-1} and 3520 cm^{-1} reflect the hydrogen bonded O-H stretching frequencies, all the other peaks areas expected for the organic moiety.

In general, arylammonium ions display a strong and broad absorption in the region of 3300–3030 cm^{-1} due to N–H stretching vibration, whereas C–N bending vibration of secondary amine appears at around 1384 cm^{-1} [15, 16] and C–C bending vibration appears at 1303 cm^{-1} . All the bands were assigned by comparison with the spectra of organic compounds [17, 18].

Table 5. Infrared frequencies (cm^{-1}) and band assignment

IR (cm^{-1})	Assignment
3800	ν_{as} (O-H)
3520	ν_{s} (O-H)
3444	ν_{as} (NH_3^+)
3314	ν_{as} (NH_2^+)
3080	ν_{s} (NH_3^+), ν_{s} (NH_2^+)
2970	ν_{as} (CH_2)
2818	ν_{s} (CH_2)
1572	δ_{s} (NH_2^+), δ_{as} (NH_3^+)
1493	δ_{s} (NH_3^+), δ_{a} (CH_2) aliphatic
1475	δ_{s} (NH_3^+), δ_{s} CH_2 aliphatic
1458	δ_{s} (NH_3^+), δ_{as} (CH_2) cyclic
1439	δ_{as} (CH_2) cyclic
1408	δ (CNH), δ (CCH), δ (NCH)



1384	$\nu(\text{C-N})$ secondary amine, $\delta(\text{CNH})$, $\delta(\text{CCH})$, $\delta(\text{NCH})$
1344	} $\delta(\text{CNH})$, $\delta(\text{CCH})$, $\delta(\text{NCH})$, $\omega(\text{CH}_2)$ and $\delta_{\text{as}}(\text{CH}_2)$ cyclic
1330	
1304	
1292	} $\tau(\text{CH}_2)$
1266	
1233	
1195	
1164	$\rho(\text{NH}_3^+)$
1136	$\nu_a(\text{C-N})$, $\tau(\text{CH}_2)$ and $\rho(\text{NH}_3^+)$
1082	$\nu_a(\text{C-C})$, $\rho(\text{NH}_2^+)$ and $\omega(\text{CH}_2)$ $\delta(\text{C-H})$ cyclic in plane
1070	$\nu_a(\text{C-C})$
1051	$\nu_a(\text{C-N})$
1039	$\delta(\text{C-H})$ out of plane; $\nu(\text{C-N})$ primary amine
998	$\rho(\text{NH}_3)$ and CH bending
953	$\rho(\text{NH}_3)$, $r(\text{NH}_3)$
942	$\rho(\text{CH}_2)$
854	} $\rho(\text{CH}_2)$
818	
800	
772	$\omega(\text{NH}_3^+)$
602	} $\nu(\text{C-C-N})$
576	

III.3. Calorimetric study

DSC experiments were performed on heating the 1(2-ammonium-ethyl) piperaziniumpentachlorothallate (III) dihydrate samples from 193 K to 373 K. The thermal analysis results are reported in figure 4. The thermogram reveals one endothermic peak at $T = 320$ K. The calculated transition enthalpy for this transition is $\Delta H = 200.14 \text{ J}\cdot\text{mol}^{-1}$. This transition was confirmed by dielectric permittivity and conductivity measurements at different frequencies and temperatures.

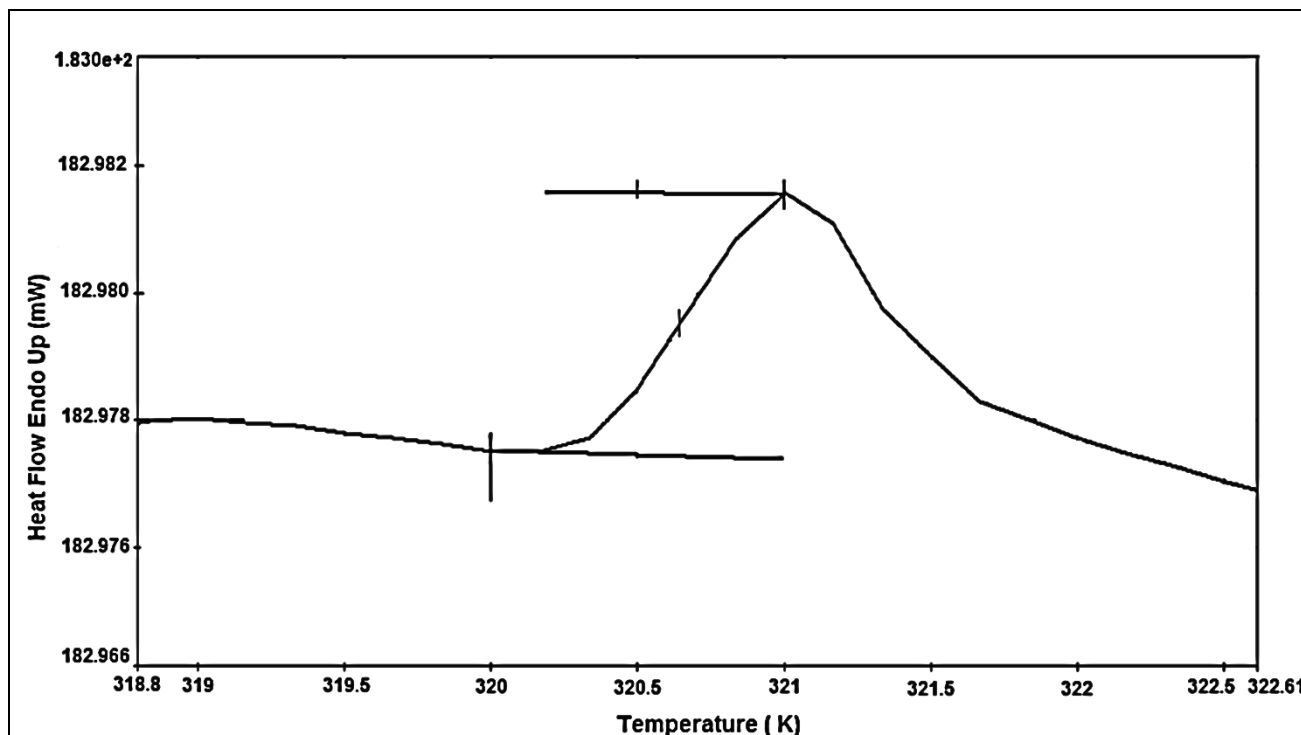


Fig 4.: Differential scanning calorimetry curve of $[\text{C}_6\text{H}_{17}\text{N}_3] \text{TiCl}_5 \cdot 2\text{H}_2\text{O}$.

III.4. Electrical study

The study of dielectric properties is an important source of valuable information about conduction processes and, in order to give more information on the crystal dynamics, we have undertaken a dielectric study between 298 and 413 K in the frequency range of 1Hz-1MHz.

Impedance spectroscopy

Complex impedance spectra Z' vs. Z'' ; [$Z''=f(Z')$] recorded at various temperatures are presented in Figure 8. As the temperature increases, the semicircles move to a lower value of resistance. So, the complex impedance spectrum shows that the title compound follows the Cole-Cole law.

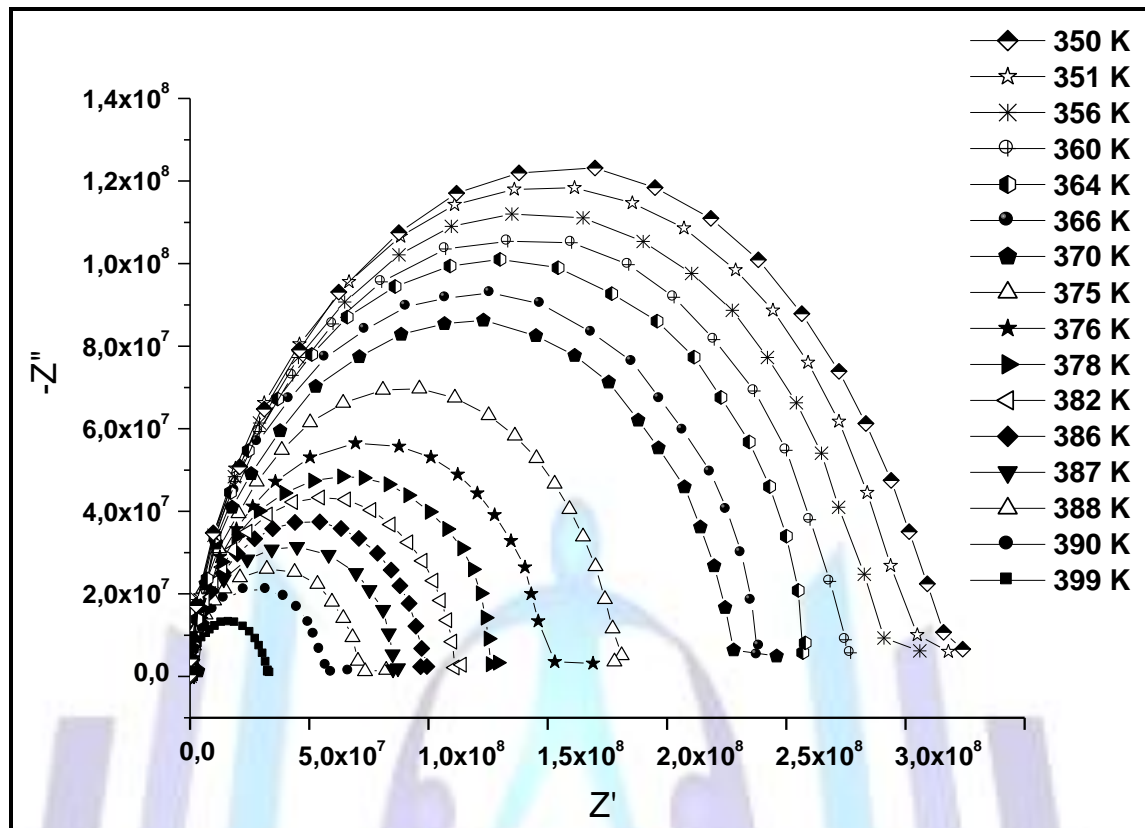


Fig 8: Complex impedance diagrams ($-Z''$ versus Z') for $[C_6H_{15}N_3] TiCl_5 \cdot 2H_2O$ at various temperatures.

The following relations were used forevaluating the various quantities. Realpart (Z') and imaginarypart (Z'') of impedance were directly measured from thebridge.

The complex dielectric constant:

$$Z^* = \frac{1}{Y^*} = \frac{1}{j\omega C_0 \epsilon^*}$$

Where $\epsilon^* = \epsilon'_r - j\epsilon''_r$

The real part of the dielectricconstant,

$$\epsilon'_r = \frac{Z''}{\omega C_0 (Z'^2 + Z''^2)}$$

The imaginary part of the dielectric constant,

$$\epsilon''_r = \frac{Z'}{\omega C_0 (Z'^2 + Z''^2)}$$

With $C_0 = \frac{\epsilon_0 S}{e}$, $\epsilon_0 = (1/36\pi) 10^{-9} \text{ F.m}^{-1}$ permittivity of the vacuum.

S and e represent respectively the surface and the thickness of the title compound. The dielectric loss or dissipation factor $\text{tg}\delta$ is the ratio $\epsilon''_r / \epsilon'_r$. The temperature dependence of the real (ϵ'_r), imaginary (ϵ''_r) of the dielectric permittivity and the dissipation factor ($\text{tan}\delta$) in the 1Hz-1MHz range of $[C_6H_{15}N_3] TiCl_5 \cdot 2H_2O$ at different frequencies is shown in figures 5, 6 and 7. These curves show one anomaly at about 320 K. As can be clearly seen, there is significant dispersion of real dielectric permittivity attributed to the phase transition detected by DSC.

The maximum of the permittivity is displaced to higher temperatures upon with increasing frequency; which is in agreement with the presence of conductivity relaxation.

From the qualitative analysis of ϵ'_r , two consecutive steps can be observed:



- The dielectric response shows anomaly around $T = 320$ K and a very large increase in permittivity above this transition. This behaviour confirms the results obtained by the DSC method.
- The permittivity ϵ_r' around T considerably increases as frequency decreases. This is in agreement with the large conductivity present in this material.

Consequently, the real part of permittivity can be considered as the summation of two contributions: the first presents the lattice response due to permanent dipole orientation, and the second is attributed to the conductivity phenomenon related to the organic cation containing π -electrons systems asymmetricized by electron donor and/or acceptor substitutes [38].

The values of dissipation factor are relatively large, in agreement with the important contribution of conductivity in this material, so the transition is characterized by a maximum of ϵ' and ϵ'' at 320 K corresponding to a maximum of $\tan \delta$. This dielectric behavior rules out the existence of a ferroelectric phase at high temperature and this transition is manifested by a strong jump in the conductivity plot. So, by increasing the temperature, as a consequence of Cl atoms disordering, the reorientation of NH_3^+ and NH_2^+ ions becomes more excited, which contributes to the high conductivity of the material [37]. This freezing is usually associated with changes in the hydrogen bonding scheme between the organic cations and the anionic groups which results in significant distortions of the latter [19–20].

This feedback between the two structural elements is responsible for the complex transition situation in this family of compounds and provides the opportunity to tailor the transition behavior and physical properties through synthesis.

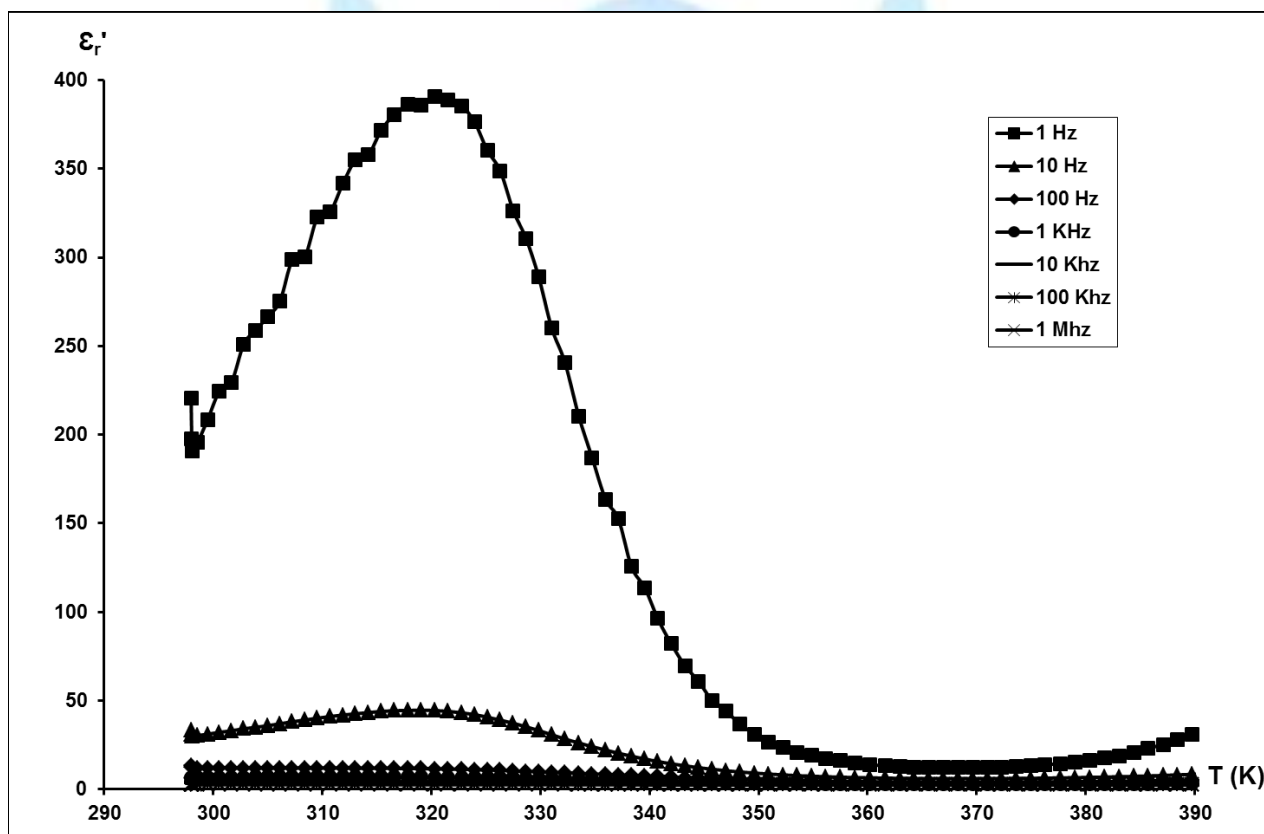


Fig 5: Temperature dependence of ϵ_r' for different frequencies for $[\text{C}_6\text{H}_{15}\text{N}_3] \text{TlCl}_5 \cdot 2\text{H}_2\text{O}$

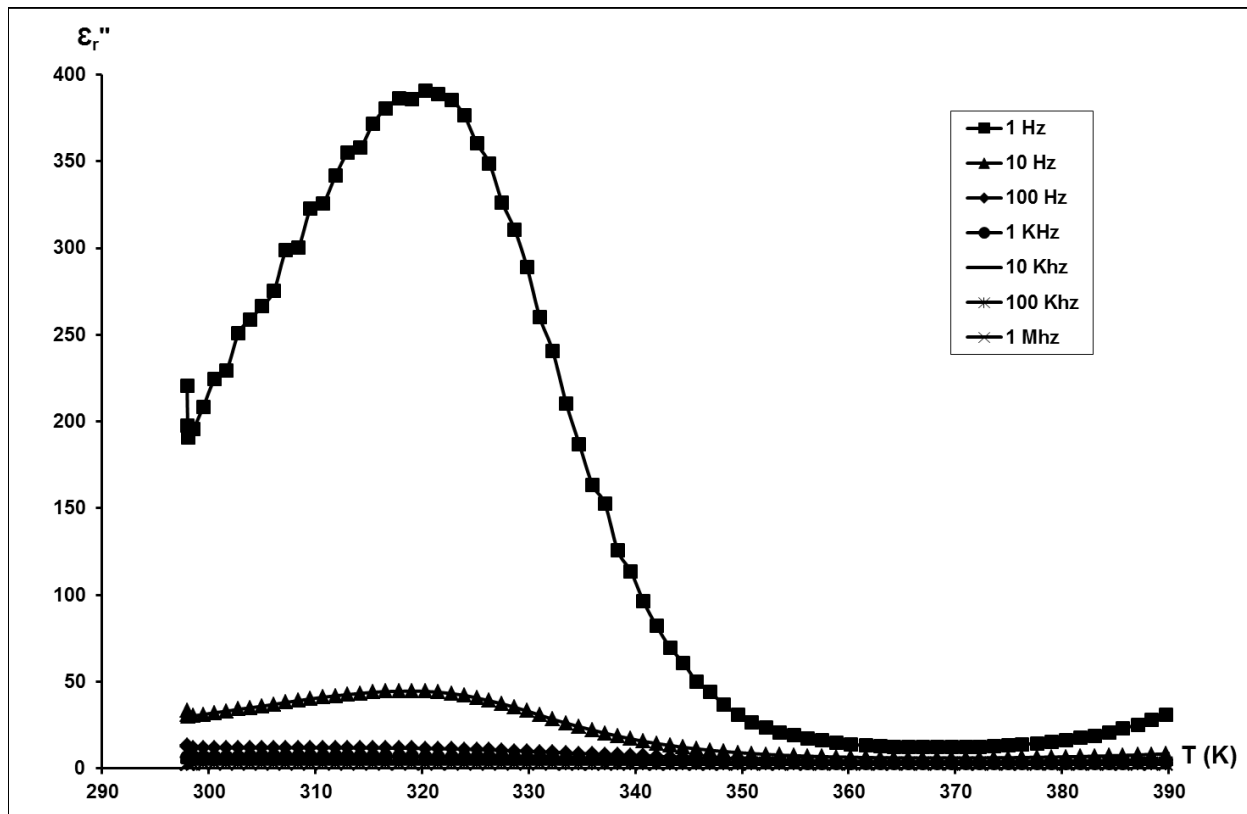


Fig 6: Temperature dependence of ϵ_r'' for different frequencies for $[C_6H_{15}N_3] TICl_5 \cdot 2H_2O$

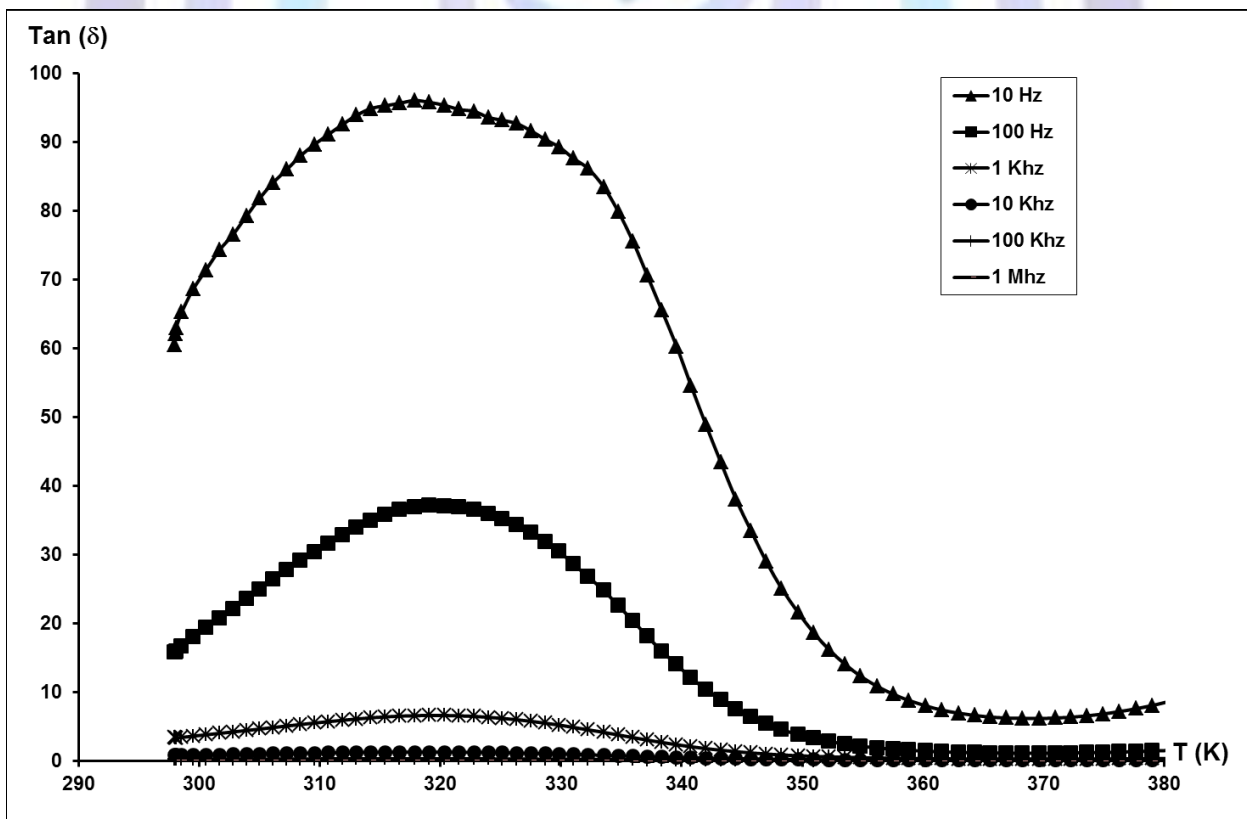


Fig 7: Temperature variation of $\tan \delta$ for $[C_6H_{15}N_3] TICl_5 \cdot 2H_2O$.



In order to understand the conduction phenomena, we used Arrhenius modeling equation: $\sigma T = A \exp(-E_a/k_B T)$, where E_a is the activation energy, A is the pre-exponential factor, k_B is the Boltzmann constant, and T is the temperature.

The thermal evolution of the specific conductivity ($\log(\sigma T)$) versus ($1000/T$) of the 1-(2-ammonium-ethyl) piperaziniumpentachlorothallate (III) is shown in Figure 9 indicating an Arrhenius-type behavior. In the 298–413 K temperature range, the conductivity plot exhibits one anomaly at 320 K. Consequently, the diagram presents two regions. The first region between 298 and 320 K and the second part of the conductivity curve between 320 and 413 K. The conductivity evolution in these regions obeys the Arrhenius law.

In comparison with studied thallium (III) compounds [9, 21], this anomaly probably corresponds to a structural phase transition, which transforms our solid solution from phase I to phase II. The activation energy values determined in the two regions I and II are respectively equal to 0.088 eV and 0.416 eV. The difference can be due to the high displacement of the ammonium proton.

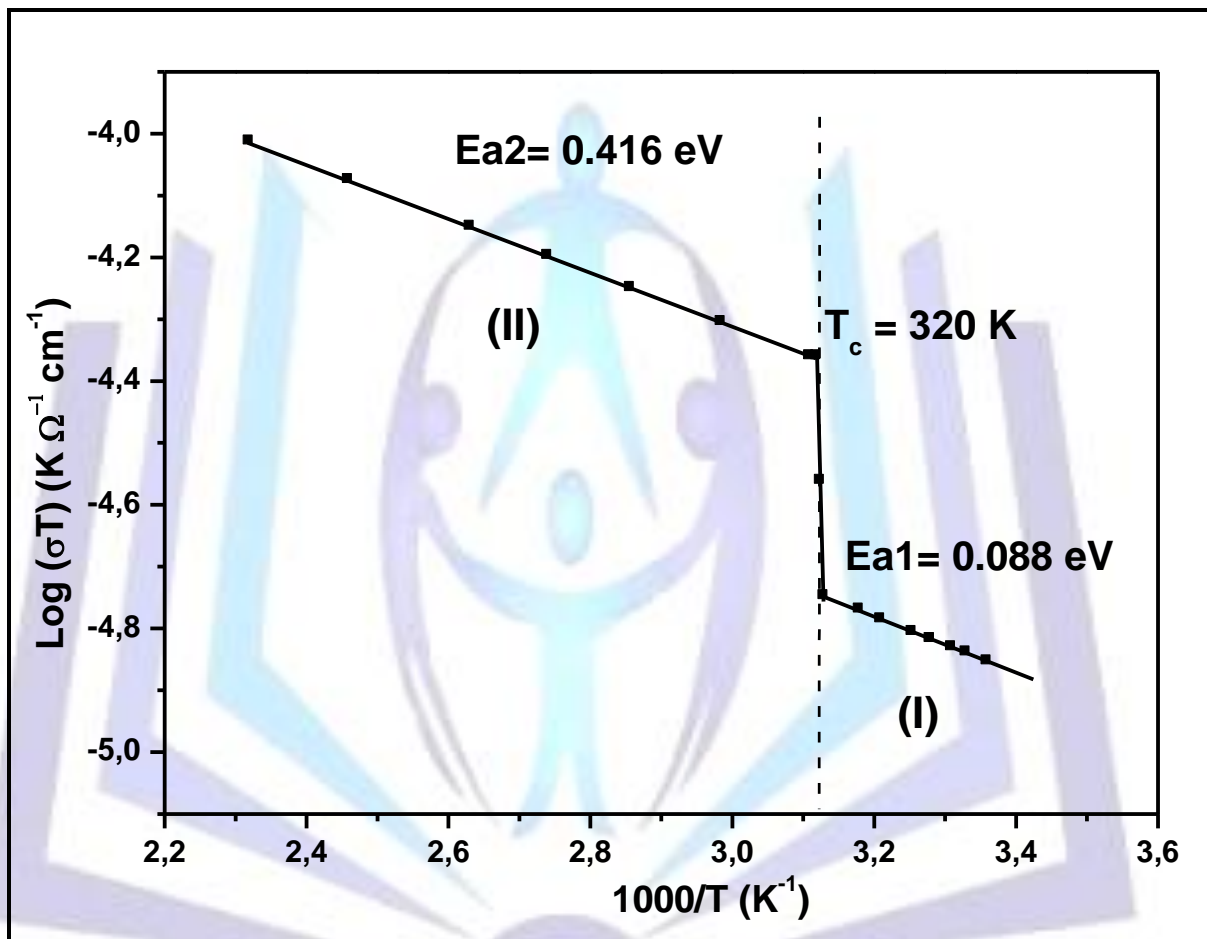


Fig 9: Conductivity plots $\log_{10}(\sigma T) = f(1000/T)$ for $[\text{C}_6\text{H}_{15}\text{N}_3]\text{TlCl}_5 \cdot 2\text{H}_2\text{O}$.

Crystallographic studies show that this material presents a noncentrosymmetric space group at room temperature which is in agreement with our last deduction. This interpretation remains to be confirmed by pyroelectric and dielectric hysteresis measurements on single crystals. This anomaly is characterized by a sharp increase in the conductivity values, the conductivity increases from $\sigma = 4.70 \cdot 10^{-8} \text{ S} \cdot \text{cm}^{-1} \cdot \text{K}^{-1}$ at 298 K to $\sigma = 2.26 \cdot 10^{-7} \text{ S} \cdot \text{cm}^{-1} \cdot \text{K}^{-1}$ at 413 K. The sudden variation of the conductivity at 320 K marks the transition.

- To more disordered state which might be correlated with changes in the orientation of molecular groups as $[\text{C}_6\text{H}_{15}\text{N}_3]$ or TlCl_5 ;
- And to the high dynamical disorder of NH_3 proton in the $\text{N-H} \dots \text{Cl}$ hydrogen bond which leads to fast proton conduction.

The conductivity here is considered to be induced by the reorientation of $[\text{C}_6\text{H}_{15}\text{N}_3]^+$ cations. By increasing the temperature, as consequence of the disordering of H atoms the reorientation of NH_2^+ and NH_3^+ ions becomes more excited which contribute to high conductivity of the material [22, 23].



Conclusion

The 1(2-ammonium-ethyl) piperaziniumpentachlorothallate (III) dihydrate belongs to the monoclinic system with Cm space group. The structure of this compound consists of $[\text{C}_6\text{H}_{17}\text{N}_3]^{2+}$ cations and a $[\text{Cl}_2\text{Cl}_{10}]^{4-}$ dimmers. These dimmers are themselves interconnected by means of the N-H... Cl hydrogen bonds.

This study has shown that the $[\text{C}_6\text{H}_{15}\text{N}_3] \text{TiCl}_5 \cdot 2\text{H}_2\text{O}$ crystal undergoes a second phase transition as a function of temperature as determined by differential scanning calorimetry, and dielectric measurement. We note the appearance of the (I→II) phase transition at $T = 320 \text{ K}$, which is of the order-disorder type. This can be explained by the conductivity phenomenon related to the organic aromatic cation containing π -electrons systems asymmetricized by electron donor and/or acceptor substitutes.

Additional studies on the nature of the phase transition (NQR and crystal structure at high temperature) are under way and will give more information on the nature of the structural phase transition.

ACKNOWLEDGEMENTS

This work was supported by the Minister Education and Research of Tunisia.

REFERENCES

- [1] T. Spiro, *Inorg. Chem.* 4 (1965) 731-738
- [2] J. Hoard, I.J. Goldstein, *Chem. Phys.* 3 (1935) 199-202.
- [3] A. Linden, A. Petridis, B.D. James, *Acta Crystallogr. C* 58 (2002)53-55.
- [4] A. Linden, B.D. James, *Acta Crystallogr. C* 58 (2002) 439-440.
- [5] A. Linden, K.W. Nugent, A. Petridis, B.D. James, *Inorg. Chim.Acta* 285 (1999) 122-128.
- [6] A. Linden, M.A. James, M.B. Millikan, L.M. Kivlighon, A. Petridis, B.D. James, *Inorg. Chim. Acta* 284 (1999) 215-222.
- [7] A. Linden, A. Petridis, B.D. James, *Inorg. Chim. Acta* 332 (2002) 61-71.
- [8] R.A. Walton, *Inorg. Chem.* 7 (1968) 640-648.
- [9] U. Geiser, J.A. Schlueter, A.M. Kini, A. Achenbach, A.S. Komosa, J.M. Williams, *ActaCrystallogr. C* 52 (1996) 159-162
- [10] G. Charlot, *Chimie Analytique Quantitative*, vol. 2, Masson et Cie, Paris, 1974
- [11] G.M. Sheldrick, *Program for Crystal Structure Determination; SHELXS-86* (1990).
- [12] G.M. Sheldrick, *Program for Crystal Structure Determination; SHELXL-97* (1997).
- [13] A. Linden, B.D. James, *Acta Cryst. C*58 (2002) 439-440.
- [14] M. Abdi, F. Zouari, S. Chaabouni, Z. Elaoud, A. Ben Salah, *Phase Transit.* 76 (2003) 723-731.
- [15] Misra SCK, Chandra S. *Indian J Chem* 1994;33A:583-594.
- [16] Silverstein RM, Webster FX. *Spectroscopic identification oforganic compounds*. 6th ed. Singapore: John Wiley & Sons, Inc; 2002.
- [17] A. Margareta, G.H. Mateescu, *Infra Red Spectroscopy*, WileyInterscience, New York, 1972.
- [18] L.J. Bellamy, *The Infrared Spectra of Complex Molecules*, Chapman and Hall, London, 1995.
- [19] R. Jakubas, L. Sobczyk, *Phase Transit.* 20 (1990) 163-193.
- [20] R. Jakubas, G. Bator, Z. Ciunik, *Ferroelectrics* 295 (2003) 3-8.
- [21] R.A. Walton, *Inorg. Chem.* 7 (1968) 640-648.
- [22] A. Kabadou, S. Walha, M. Mnif, R. Ben Hassen, A. Ben Salah, *Solid State Ionics* 122 (1999) 263-269.
- [23] A. Kabadou, R. Ben Hassen, A. Ben Salah, T. Jouini, *Status Solidi* 208 (1998) 387-395.